The Astrophysical Journal Supplement Series, 235:6 (11pp), 2018 March https://doi.org/10.3847/1538-4365/aaa1a5

The Updated Multiple Star Catalog

Andrei Tokovinin
Cerro Tololo Inter-American Observatory, Casilla 603, La Serena, Chile; atokovinin@ctio.noao.edu
Received 2017 October 23; revised 2017 December 10; accepted 2017 December 11; published 2018 February 23

Abstract

The catalog of hierarchical stellar systems with three or more components is an update of the original 1997 version. For 2000 hierarchies, the new Multiple Star Catalog (MSC) provides distances, component masses and periods, and supplementary information (astrometry, photometry, identifiers, orbits, notes). The MSC content and format are explained, and its incompleteness and strong observational selection are stressed. Nevertheless, the MSC can be used for statistical studies and is a valuable source for planning observations of multiple stars. Rare classes of stellar hierarchies found in the MSC (with six or seven components, extremely eccentric orbits, planar and possibly resonant orbits, hosting planets) are briefly presented. High-order hierarchies have smaller velocity dispersion compared to triples and are often associated with moving groups. The paper concludes with an analysis of the ratio of periods and separations between inner and outer subsystems. In wide hierarchies, the ratio of semimajor axes, estimated statistically, is distributed between 3 and 300, with no evidence of dynamically unstable systems.

Key words: binaries: close – binaries: general – binaries: visual

Supporting material: machine-readable tables

1. Introduction

This paper contains a collection of observational data on hierarchical multiple stars and updates the Multiple Star Catalog (MSC; Tokovinin 1997). The usefulness of this compilation is supported by 210 citations to the original paper. Hierarchical stellar systems are interesting for several reasons: as clues to the formation mechanisms of multiple stars, as sites of interesting dynamical phenomena, and as progenitors of some rare products of stellar evolution like blue stragglers. Recent discoveries of planets in hierarchical systems have generated additional interest in these objects and are a stimulus to understand the common origin and evolution of stellar and planetary systems.

The content of the MSC results from random discoveries and gives a distorted reflection of the real statistics in the field. However, volume-limited samples (e.g., Raghavan et al. 2010) are necessarily small and contain only a modest number of hierarchies, diminishing their statistical value. For solar-type stars, an effort to extend the distance limit to 67 pc while still controlling the observational selection was made by Tokovinin (2014) and has led to the first reliable estimate of the frequency of various hierarchies in the field. But even this volume-limited sample of ∼500 hierarchies is too small for finding the rarest and most interesting objects, such as close tertiary companions orbiting *Kepler* eclipsing binaries (EBs). Hence the utility of this compilation.

Like its predecessor, the updated MSC can be a source of observational programs related to multiple stars. For example, visual binaries with spectroscopic subsystems can be selected for observations with long-baseline interferometers to determine the orientations of the inner orbits and the character of dynamical evolution (Muterspaugh et al. 2010). Tertiary components can be monitored spectroscopically to detect subsystems or planets. Although the MSC does not represent a clean, volume-limited sample, some statistical inferences can nevertheless be made using this catalog.

The nature of the data incorporated into the MSC is briefly outlined in Section 2. The structure and content of the MSC are explained in Section 3. Section 4 is a tour of the multiple-star "zoo," highlighting specific members of this class. In Section 5 one statistical aspect of the MSC, namely the ratio of periods and separations, is presented. The paper concludes with a short discussion in Section 6.

2. Data Sources and Restrictions

2.1. Recent Literature

The MSC was last updated in 2010, stimulated by the work of Eggleton (2009) on the multiplicity of bright stars. However, more than half of the hierarchical systems within 67 pc (Tokovinin 2014) were discovered after 2010. So, as a first step, those nearby hierarchies were added to the MSC, and its format has been slightly changed in the process.

The updated MSC reflects the results of the large multiplicity surveys of the last decade, ranging from low-mass and substellar systems in the solar neighborhood (Law et al. 2010; Dieterich et al. 2012) to A-type stars within 75 pc (De Rosa et al. 2014) and massive O-type stars beyond 1 kpc (Sana et al. 2014). New hierarchies have also been discovered by speckle interferometry (e.g., Tokovinin et al. 2010).

Precise photometry from space furnished by the *Kepler* and *COROT* satellites has led to the discovery of thousands of EBs. Some of those EBs show cyclic variations of eclipse time and/or a precession caused by relatively close tertiary components (Borkovits et al. 2016). About 200 such new compact triple systems have been added to the MSC. Ongoing searches of exoplanets by radial velocity and transits also contributed new hierarchical systems, some of them containing planets.

2.2. Data Mining

Nowadays, targeted surveys are supplemented by the large body of all-sky catalogs available online for data mining. The updated MSC contains only about 2000 systems, still a tiny number by modern standards. Its content relies on the four major catalogs of binary stars presented below, namely WDS,

INT4, VB6, and SB9. These catalogs are frequently updated, so we used their recent (2016) online versions.

The Washington Double Star Catalog (WDS; Mason et al. 2001) lists thousands of resolved stellar systems with two, three, or more components. However, a substantial fraction of WDS entries are random combinations of background stars (e.g., optical pairs). Almost any bright star has faint optical components in WDS. Optical pairs are more frequent in crowded regions of the sky; typically their secondary components are faint. Real (physical) pairs with substantial proper motion (PM) can be distinguished from the optical ones (see Section 3.6). This naturally favors nearby and low-mass stars, while the nature of distant and massive visual double stars with small PMs remains uncertain. Moreover, several "multiple systems" with common PMs found in WDS are simply groups of stars belonging to the same cluster. Apart from the optical pairs, WDS contains spurious pairs that have not been confirmed by subsequent observations. For example, many Tycho binaries (discovery codes TDS and TDT) with separations on the order of 0.″5 are spurious because they are not confirmed by speckle interferometry.

Considering this "noise," no attempt to extract triple systems from WDS has been made in the original MSC compilation. In this version, candidate triples with PMs above 50 mas yr^{-1} were selected from WDS automatically. Some of them passed the reality test and were added to the new MSC. The Fourth Catalog of Interferometric Measurements of Binary Stars (INT4; Hartkopf et al. 2001) was consulted in the process.

Hierarchical systems with known orbits are of special interest. Entries of the Sixth Catalog of Visual Binary Orbits (VB6; Hartkopf et al. 2001) were cross-checked with WDS for the presence of additional physical components. Similarly, the Ninth Catalog of Spectroscopic Binary Orbits (SB9; Pourbaix et al. 2004) was matched with WDS. This data mining has improved the census of triple systems among "orbital" binaries. The number of those binaries is steadily growing, while not all of them are featured in SB9 and VB6. Therefore, scanning the current literature is an essential complement to the data mining.

2.3. Limitations

The vast majority of hierarchical systems in the MSC are located within 1 kpc from the Sun. Nearby objects are generally brighter and have the advantage of being resolvable; their large PMs help to get rid of optical companions. Although modern observations go very deep and far, we decided to ignore hierarchies in the Magellanic clouds and beyond, as well as many distant massive stars.

Some EBs have periodic eclipse time variations (ETVs) that can be explained either by the presence of a tertiary component or by magnetic cycles in one or both components of the eclipsing pair (see the discussion in Liao & Quian 2010). In many cases the existence of tertiary components is confirmed by other methods (e.g., J02091+4088 or BX And, where the 62-year tertiary has an astrometric orbit). On the other hand, some tertiary components discovered by ETV remain controversial. For example, Zhou et al. (2016) claimed that J01534+7003 (V776 Cas) is a quadruple system, based of the ETV with a period of 23.7 yr, of which one cycle is observed. The implied tertiary component of one solar mass with a fractional luminosity of 0.15 should be detectable in the spectrum. Yet, D'Angelo et al. (2006) found only a weak spectral signature, with a fractional luminosity of 0.015 corresponding to the visual companion B at 5.″4 separation. Accordingly, V776 Cas is listed in the MSC as triple rather than quadruple, until the reality of the 23.7 year subsystem is confirmed. It is noteworthy that tertiary components found by ETV usually have circular orbits, while typical binary orbits have non-zero eccentricity. We leave aside many triple systems discovered by ETV until they are confirmed by other techniques.

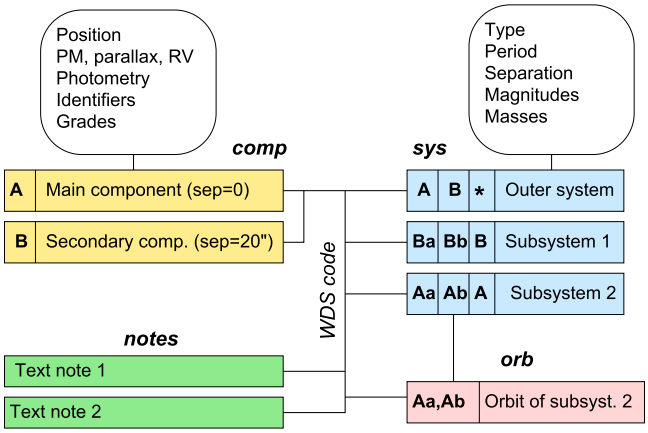

Figure 1. Structure of the MSC. It consists of four tables, `comp`, `sys`, `orb`, and `notes`, linked by the WDS code, unique for each multiple system.

For most systems, the MSC does not provide bibliographic references. Given the coordinates and/or common identifiers, the bibliography can be retrieved from Simbad. Information on resolved binaries is retrieved from WDS and INT4, and the orbital elements are sourced from VB6 and SB9. The notes give references where appropriate, e.g., for subsystems that are not found in the main catalogs. Additional parameters such as masses and periods are estimated by the methods explained below.

3. The New MSC

3.1. Catalog Structure

The structure of the MSC was described in the original paper (Tokovinin 1997); it changed only slightly. The MSC consists of four tables linked by the common field based on WDS-style coordinates for the J2000 epoch (Figure 1). We call them WDS codes, although, strictly speaking, the equivalence applies only to the resolved visual binaries actually listed in WDS. The tables are available in full as text files. They are too wide to fit on the printed page, therefore providing their fragments would not be useful to the reader. Instead, we describe the content of each table. The format codes indicate the types of the fields in the machine-readable tables (A—string, F—floating number, I—integer number).

Part of the MSC content is available in the online database that allows searches for identifiers or coordinates.[1] The same link also leads to the full ASCII tables and old versions of the MSC.

Illustrating the MSC content, Figure 2 plots its distribution on the sky in equatorial coordinates. The cluster of points at (290°, +50°) corresponds to multiple systems in the *Kepler* field. Even without those multiples, the number of systems with northern declinations is larger than the number of southern

[1] http://www.ctio.noao.edu/~atokovin/stars/

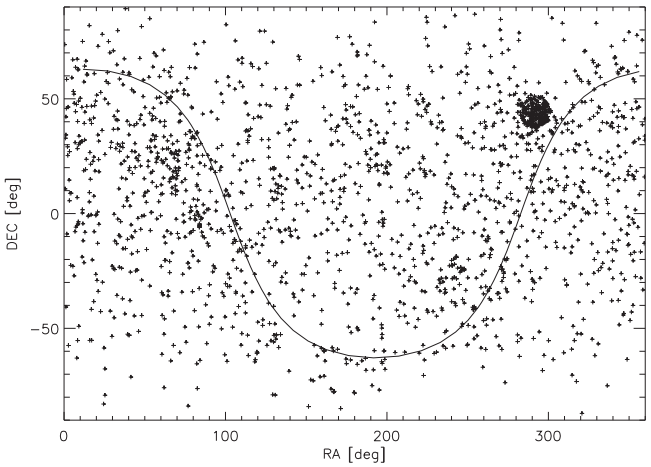

Figure 2. Distribution of the MSC objects in the sky. The line shows the Galactic equator.

multiples, reflecting the historical bias in favor of the northern sky.

Figure 3 illustrates the dependence of the MSC content on the distance d; the median distance is 113 pc. The upper plot shows strong correlation of the primary mass with the distance; only a few low-mass multiples are discovered beyond 30 pc. Not surprisingly, the number of objects in the MSC is not proportional to d^3, as one might expect for a spatially uniform population. Instead, the d^2 law is a good fit to the cumulative counts at $d < 50$ pc. When the range of masses is restricted to solar-type stars, the d^2 law still holds well, demonstrating incompleteness of the MSC even for those well-studied objects. The lower plot of periods versus distance gives evidence of a "gap" at $P \sim 100$ days, possibly a selection effect. The lack of long periods (wide binaries) beyond ∼300 pc is also obvious; such binaries have small PMs and are not discovered by the current surveys. The *Kepler* EBs with tertiary components and outer periods around 1000 days make a distinct group at the distance of ∼1 kpc. The plots in Figure 3 give an idea of the "typical" hierarchical system: it has a primary mass between 0.5 and 3 $\mathcal{M}_\odot$ and is located within 300 pc from the Sun.

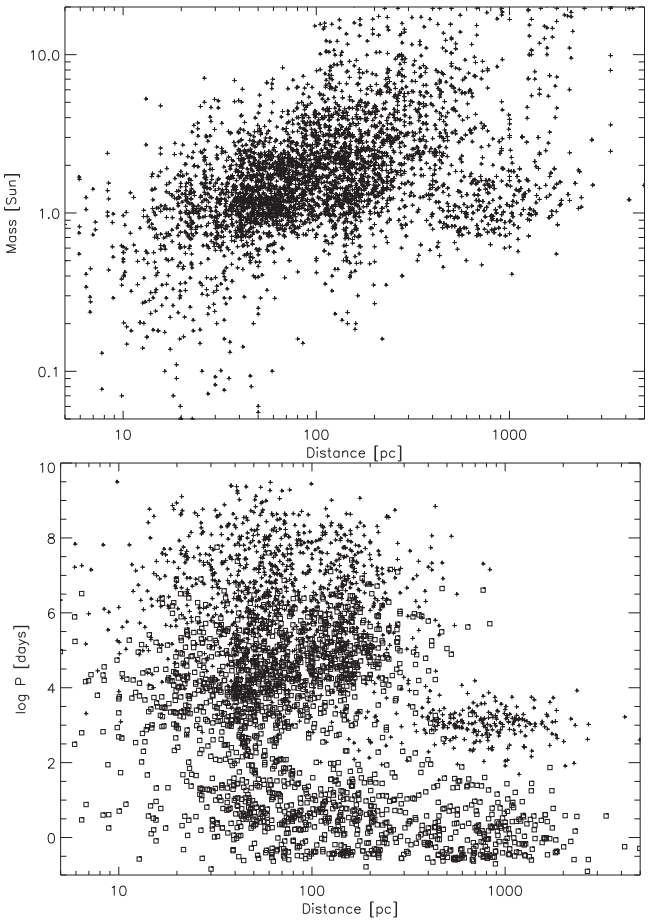

Figure 3. MSC content vs. distance. Top: primary mass vs. distance. Bottom: periods vs. distance for primary mass less than 3 $\mathcal{M}_\odot$ (crosses—outer periods, squares—inner periods).

3.2. Components Table (comp)

The main table `comp` contains data on the individual components, both primary and secondary: astrometry, photometry, and identifiers (see Table 1). The MSC does not provide the errors for astrometry or photometry, as these data are recovered from various heterogeneous sources; it should not be used as an astrometric or photometric catalog.

The brightest star in each multiple system—its primary component—always has an entry in the `comp` table. Other components with separations larger than a few arcseconds from the primary, if present, have their own entries. The non-zero separation distinguishes them from the primaries. To count multiple systems, only primary components with zero separation should be considered. However, photometry, astrometry and identifiers of the secondary components, when available, are very useful for evaluating their relation to the primary and for compilation of observing programs.

The unknown (missing) parameters in the MSC have zero values. This feature is inherited from the original MSC and should be kept in mind when using the tables.

The MSC provides the HD and HIP numbers for locating the stars in the SIMBAD. However, the objects in the new MSC are, on average, fainter than those in the old one, and an increasing fraction of them (especially the secondary components) lack traditional identifiers. On the other hand, faint stars may have a variety of useful aliases, e.g., *Kepler* or 2MASS numbers, variable-star designations, etc. In response to this situation, the new MSC contains a collection of arbitrary identifiers in free format. Coordinates and identifiers help to retrieve information on components from *Vizier* or other sources.

3.3. Systems Table (sys)

The table `sys` contains information on the individual subsystems: their types, periods, separations, and masses (see Table 2). The fields *primary*, *secondary*, and *parent* contain components' identities and jointly describe the hierarchical structure. This is illustrated in Figure 4 using the sextuple system Castor as an example. The outer hierarchical level (root) is the wide binary AB, C,* consisting of the components AB and C (the root is coded by the asterisk in the parent field). The component C is a close spectroscopic binary. The system A,B is a visual binary with a period of 445 yr. In turn, both its components A and B are close spectroscopic binaries. So, a component of the hierarchy may contain several stars. To avoid confusion, in most cases the component designations in the MSC match those in WDS, although arbitrary character strings

Table 1
Components Table (comp)

Field	Format	Description
WDS	A10	WDS code (J2000)
RA	F10.5	Right ascension J2000 (degrees)
DEC	F10.5	Declination J2000 (degrees)
Parallax	F8.2	Parallax (mas)
Refplx	A4	Reference code for parallax[a]
PMRA	F7.1	Proper motion in R.A. (mas yr^{-1})
PMDE	F7.1	Proper motion in decl. (mas yr^{-1})
RV	F6.1	Radial velocity (km s^{-1})
Comp	A2	Component label
Sep	F7.1	Separation (arcseconds)
Sp	A8	Spectral type
HIP	I6	*Hipparcos* number
HD	I6	HD number
Bmag	F5.2	*B*-band magnitude
Vmag	F5.2	*V*-band magnitude
Imag	F5.2	I_C band magnitude
Jmag	F5.2	*J*-band magnitude
Hmag	F5.2	*H*-band magnitude
Kmag	F5.2	*K*-band magnitude
Ncomp	I2	Number of physical components
Grade	I1	Grade[b]
Ident	A40	Other identifiers

Notes.
[a] Parallax codes: HIP—*Hipparcos*, *Gaia*—*Gaia* DR1, dyn—dynamical, orb—orbital, pN—photometric from component N, bib—taken from the literature.
[b] See Section 3.7.

(This table is available in its entirety in machine-readable form.)

Table 2
Systems Table (sys)

Field	Format	Description
WDS	A10	WDS code (J2000)
Primary	A3	Primary component label
Secondary	A3	Secondary component label
Parent	A3	Parent label[a]
Type	A6	Observing technique/status[b]
P	F10.4	Orbital period
Punit	A1	Units of period[c]
Sep	F8.3	Separation or semimajor axis
Sepunit	A1	Units of separation[d]
Pos. angle	F5.1	Position angle (deg)
Vmag1	F5.2	*V*-band magnitude of the primary
Sp1	A5	Spectral type of the primary
Vmag2	F5.2	*V*-band magnitude of the secondary
Sp2	A5	Spectral type of the secondary
Mass1	F6.2	Mass of the primary (Sun)
Mcode1	A1	Mass estimation code for Mass1[e]
Mass2	F6.2	Mass of the secondary (Sun)
Mcode2	A1	Mass estimation code for Mass2[e]
Comment	A20	Comment on the system

Notes.
[a] Parent points to the component identifier in the higher-level system to which the current system belongs and thus codes the hierarchy by reference. Two special symbols are used: * means the root (system at the highest hierarchical level); and t means a trapezium-type, non-hierarchical system.
[b] See Table 3.
[c] Period units: d—days, y—yr, k—kyr, M—Myr.
[d] Separation units: ″—arcseconds, ′—arcminutes, m—mas.
[e] Mass codes: r—given in the original publication, v—estimated from absolute magnitude, a—estimated from spectral type or color index, s—sum of masses for the subsystem(s), q—estimated from primary mass and the mass ratio of SB2, m—minimum secondary mass for SB1.

(This table is available in its entirety in machine-readable form.)

can be used as component designations just as well, and there are no strict rules here. For example, a resolved secondary can be designated as Ba,Bb,B, or as B,C,BC both in the MSC and in WDS. Systems are designated by their primary and secondary component (and, sometimes, root), joined with a comma. This notation is explained in Tokovinin (2005) and Tokovinin et al. (2006).

Although the MSC contains predominantly hierarchical stellar systems, in several cases the separations between resolved components are comparable and it is not known if those systems are hierarchical or not. Such apparently non-hierarchical configurations are called *trapezia*. In the MSC, trapezia are denoted by the symbol "t" in the parent field instead of the usual "*." Thus, a trapezium has two or more upper-level systems with the parent "t," but no root system. Note that the Orion Trapezium that gave name to this class of objects is in fact a young stellar cluster. We do not consider it as a single entry, but include three hierarchies belonging to the Orion Trapezium as separate entries, each with its own WDS code.

The types of the systems reflect the discovery techniques, with an obvious coding: C—common proper motion (CPM; see Section 3.6), v—visual, etc. (see Table 3). A system can have several types, e.g., a resolved spectroscopic binary has types v and s (or V and S if both visual and spectroscopic orbits are known). The special type X denotes optical or spurious systems that are kept in the `sys` table only for completeness.

The type defines the meaning of the period and separation. For systems with known orbits (types A, V, S, E), those fields contain the actual period and the semimajor axis a in

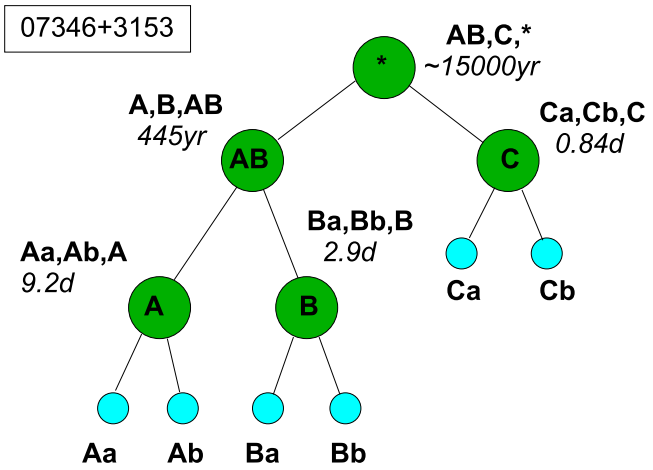

Figure 4. Hierarchical structure of the sextuple system Castor (J07346+3153, α Gem). The large green circles depict subsystems (their designations and periods are given), and the small blue circles denote individual stars.

angular units. For resolved binaries without known orbits, the separation ρ is listed in place of the semimajor axis, while the period P^* is estimated from the third *Kepler* law by assuming that the projected separation equals the semimajor axis:

$$P^* = (\rho/p)^{3/2} M^{-1/2}, \quad (1)$$

Table 3
System Types

Type	Discovery Technique
C[mhrp]	CPM pair and criteria of relation
c	Wide pair with uncertain status
v, o	Resolved visual or occultation binary
V	Visual binary with known orbit
a	Acceleration binary
A	Astrometric binary with known orbit
s, s2	Spectroscopic binary (e.g., double-lined)
S1, S2	Spectroscopic binary with known orbit
e, E	Eclipsing binary
E*	Eclipse time variations
X[mhrp]	Spurious pair (e.g., optical)

where M is the mass sum in solar units, p is the parallax, and P^* is in years. The ratio a/ρ is a random variable with a median value close to one and a typical variation by a factor of two around the median (Tokovinin 2014). Therefore, the estimated periods P^* are typically within a factor of 3 from the true periods. The same formula (1) is used to compute the semimajor axis of close (unresolved) binaries with known periods. Unknown periods or separations have the default zero value.

3.4. Orbits and Notes

The third table `orb` (see Table 4) lists elements of visual, spectroscopic, or combined orbits, when available. They are copied mostly from the catalogs of visual and spectroscopic orbits, VB6 (Hartkopf et al. 2001) and SB9 (Pourbaix et al. 2004), respectively, with some additions from recent literature. For unpublished spectroscopic orbits by D. Latham (2012, private communication), only periods are given in the `sys` table, with the "CfA" reference in the comment field.

Finally, the table `notes` contains notes (Table 5) in the free-text format. The new field `bibcode` is added to provide the source of some notes. However, in most cases it remains empty (we made no effort to provide bibcodes for references that are given in the old MSC in free format). The notes amply use abbreviations (e.g., plx for parallax, PM for proper motion, etc.) and short codes for common references, such as R10 for (Raghavan et al. 2010). A list of such references is given in Tokovinin (2014, Table 1).

3.5. Masses and Distances

When the first version of the MSC was compiled, the distances to most objects were not measured directly, but rather estimated from photometry and/or spectral types. Knowledge of distance and mass is needed to evaluate the period from the projected separation, or vice versa. Now the situation has changed radically, as the distances to most hierarchies are measured by *Hipparcos* (van Leeuwen 2007) and *Gaia* DR1 (Gaia Collaboration et al. 2016); the new MSC contains about 900 parallaxes from each of those sources. However, *Gaia* does not give parallaxes for stars that are either too bright or non-single, that are not yet processed in the DR1. The DR1 catalog also provides relative positions of some binaries useful for evaluating their motion.

The masses of the main-sequence components can be estimated from their absolute magnitudes more reliably than from the colors or spectral types. This is now the preferred method. We use the tabulation of Pecaut & Mamajek (2013), valid for spectral types later than O9V. Uncertain masses evaluated from the spectral types are retained only for some stars. For objects without trigonometric or dynamical parallaxes, we evaluate the absolute magnitude either from the spectral type or from the $V-K$ color (assuming a single main-sequence star without extinction) and hence derive the photometric distance. Dynamical parallaxes estimated from the visual orbits can be more accurate than photometric or even trigonometric parallaxes. When all methods fail, a rough guess of the distance is made. Estimates of masses and distances as given in the literature, whenever available, are preferred to our own estimates.

If the `comp` table has several entries for the same system, the distances to the secondary component are assumed to be the same as those for the primary, unless independent measurements for those components are available.

As a consistency test, Figure 5 compares the known trigonometric parallaxes with the dynamical parallaxes computed from the visual orbits and the estimated masses. Only orbits of grade 4 or better are used, and the comparison is restricted to parallaxes of less than 50 mas. The 144 binaries with *Hipparcos* parallaxes have a mean difference $p_{\rm HIP}-p_{\rm dyn}$ of −0.001 mas and an rms scatter of 1.98 mas. For the 23 binaries with *Gaia* parallaxes, the mean difference is −0.06 mas and the scatter is 2.57 mas. The near-zero average difference proves that the mass estimates in the MSC are unbiased. Inspection of the discrepancies suggests they come

Table 4
Orbit Table (orb)

Field	Format	Description
WDS	A10	WDS code (J2000)
System	A8	Primary, Secondary labels
P	F12.4	Orbital period (see Punit)
T_0	F10.4	Periastron epoch[a]
e	F6.3	Eccentricity
a	F8.4	Semimajor axis (arcseconds)
Ω	F6.2	P.A. of the ascending node (deg)
ω	F6.2	Argument of periastron (deg)
i	F6.2	Inclination (deg)
K_1	F6.2	Semi-amplitude of the primary (km s^{-1})
K_2	F6.2	Semi-amplitude of the secondary (km s^{-1})
V_0	F8.2	Center-of-mass velocity (km s^{-1})
Node	A1	Component to which the node refers
Punit	A1	Unit of period (days or years)
Comment	A30	Note (may include bibcode)

Note.
[a] Besselian year if P in years, JD−24,00000 if P in days.

(This table is available in its entirety in machine-readable form.)

Table 5
Notes Table (Notes)

Field	Format	Description
WDS	A10	WDS code (J2000)
Text	A80	Text of the note
Bibcode	A19	Bibcode

(This table is available in its entirety in machine-readable form.)

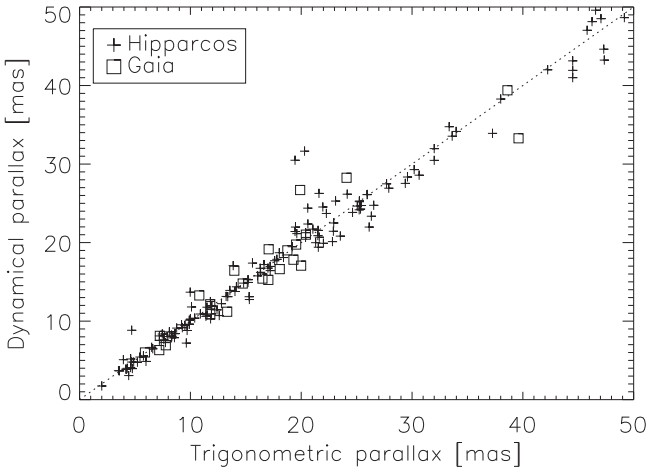

Figure 5. Comparison of trigonometric and dynamical parallaxes. The dotted line shows the equality of parallaxes.

from questionable visual orbits (even some orbits of grade 3), rather than the errors of the masses or parallaxes.

3.6. Physical or Optical?

Most visual binaries wider than 1″ have the type "*C*," meaning CPM. Several classical methods are used to distinguish real (physical) components from chance projections (optical). In the `sys` table, each method has its corresponding flag after the letter C. The similarity of PMs, flag "m," is a useful indicator when the PMs are large enough (say >30 mas yr^{-1}) to distinguish both stars from the background. Several systems with small PMs, listed in the original MSC as physical, turned out to be chance projections. A related criterion uses the relative angular motion between the components μ (in mas yr^{-1}). Bound binaries cannot move too fast. This condition can be expressed as a limit on the parallax p,

$$p > p_{\rm crit} = (\rho\mu^2)^{1/3}(2\pi)^{-1/3}M^{1/3}, \quad (2)$$

where M is the mass sum in solar units (see, e.g., Tokovinin & Kiyaeva 2016). This equation can be re-cast as the upper limit $\mu_{\rm crit}(p, M)$. Simulations show that the typical projected relative velocity is $\sim 1/3$ of its critical value $\mu_{\rm crit}$ given by (2). This leads to a statistical estimate of the parallax of $p \approx 0.26(\rho\mu^2 M)^{1/3}$, similar to the hypothetical parallax in the sense of Ressell & Moore (1940), $p_{\rm h} = 0.418(\rho\mu^2)^{1/3}$. Considering the randomness of the instantaneous orbital motions and the inevitable measurement errors of μ, the hypothetical parallax must not exceed the actual parallax by more than three times, as a rule of thumb. This criterion, denoted by the flag "h," depends on the accuracy of the relative positions used to compute μ, as well as on the time base. Unfortunately, the measurements listed in WDS (especially the first ones) can be inaccurate, compromising this criterion. We evaluate subjectively if the observed displacement of the binary reported in WDS is real, and if so, use the hypothetical parallax to reject optical pairs that move too fast. Uncertain pairs have a question mark in the type field.

Relative positions of wide pairs are not measured or cataloged with sufficient accuracy to evaluate their slow relative motion, making the hypothetical parallax useless. However, when the PM is large and the relative displacement between the first and the last measurements is much less than that implied by the PM, the stability of the relative position indicates that the pair is physical. Such cases are also denoted by the flag "h."

Common RV (flag "r") is another independent criterion of a physical binary. It can be falsified by large measurement errors or by the presence of spectroscopic subsystems. Finally, the common distance of both components (flag "p"), estimated usually from photometry, is an additional indicator of a physical relationship. When accurate parallaxes of both components are measured, this criterion is very reliable. Real physical pairs usually fulfill several criteria simultaneously.

Very wide pairs with common PMs are not necessarily gravitationally bound. Instead, they can be members of moving groups or dissolving clusters. There is no clear distinction between bound and co-moving pairs, at least observationally. In the MSC, we consider binaries with periods longer than $\sim$2 Myr (separations $>$20 kau) as potentially unbound.

3.7. Grading

The amount and quality of the information on hierarchical systems in the MSC is variable; even the existence or status of some companions is uncertain. In the new MSC we introduce a grading system analogous to the grades assigned traditionally to visual and spectroscopic orbits. The grades are found in the `comp` table, for primary components only. The integer grade numbers have the following meaning:

0. The grade is not assigned (all secondary components have grade zero).
1. Not a hierarchical system (e.g., a simple binary with false claims of additional components).
2. Either the triple nature is doubtful, or the widest companion has a very long period (typically longer than 2 Myr), being, for example, a co-moving member of a young group rather than a genuine bound companion on a Keplerian orbit.
3. Some periods are not known (e.g., a binary discovered from astrometric acceleration) or the distance is uncertain.
4. Certainly hierarchical systems with all periods known or estimated.
5. Good-quality systems with a distance accuracy of better than 10% and at least one known orbit.

There are 148 systems of grade 1 (simple binaries), 344 questionable hierarchies of grade 2, 252 systems of grade 3, 1168 of grade 4, and 705 of grade 5. The total number of hierarchical systems with grades 3 and above is 2125. These numbers change when the MSC is updated.

4. The Zoo of Multiple Stars

A catalog like MSC always contains some unusual objects. Although the MSC is burdened by large and uncertain discovery biases, the presence of rare systems in the catalog proves their existence in nature. In this section we highlight some interesting classes of hierarchical systems.

4.1. Sextuples and Seventuples

The updated MSC contains 17 systems with 6 components (4 of them are trapezia) and 4 systems with 7 components (including 1 trapezium). High-order hierarchies are difficult to

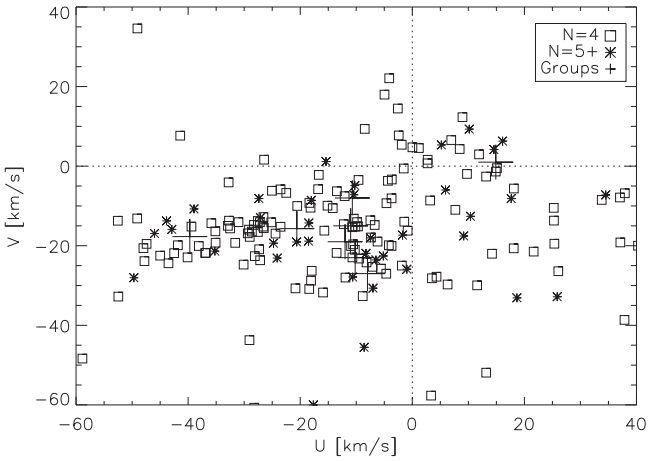

Figure 6. Kinematics of high-order hierarchies. The large crosses show the Galactic velocities of moving groups.

discover, therefore these numbers should not be used to evaluate their true relative frequency.

Among the three hierarchies with seven components, none are certain. The most reliable case is J11551+4629 (65 UMa), but its widest pair, A,D, at 63.″2, although definitely related, may represent two subsystems in a moving group, rather than a genuine bound binary (its estimated period is 0.5 Myr). The subsystem Da,Db was resolved only once in 2009 and has not been confirmed yet. The 65 UMa system is unique in having four hierarchical levels: the wide CPM pair has a 3.″9 visual subsystem that contains a 641-day spectroscopic binary with a 1.73-day eclipsing primary (Zasche et al. 2012).

Some sextuples also have either unconfirmed subsystems or uncertain status, but several sextuples are genuine. One of those, Castor (J07346+3153), is featured in Figure 4. The system J04357+1010 (88 Tau) has the same hierarchical structure as Castor and is also certainly sextuple. The young sextuple J00315−6257 (β Tuc) contains only resolved subsystems (no spectroscopic binaries); it belongs to the Tucana moving group, making the status of its widest 544″ pair (period ∼1 Myr) questionable; it can be just a pair of the moving group members.

The fact that many high-order hierarchies are members of moving groups may be significant. Compared to the field, moving groups have a larger multiplicity fraction ϵ (e.g., Elliott & Bayo 2016; Tokovinin 2017b). The frequency of hierarchies independently assembled from N subsystems is proportional to ϵ^N, hence for large N they should be produced predominantly in the high-multiplicity environment. Of course, assembly of hierarchies from independent subsystems is just a hypothesis.

Using data from the `comp` table, we computed Galactic velocities U, V, W for 866 hierarchies of grade 3 or higher located within 100 pc from the Sun. Figure 6 illustrates the kinematics of high-order hierarchies and their likely association with moving groups. The velocity dispersion in all three coordinates decreases with the increasing multiplicity order (Table 6). One might think that high-order hierarchies survive predominantly in sparse regions where the moving groups likely form. However, as Table 6 shows, the velocity dispersions of wide and compact hierarchies are statistically similar. The average velocity differences with the nearest moving group for the wide ($P_{\rm out} > 10^7$ days) and close ($P_{\rm out} < 10^4$ days) hierarchies are the same, 24.7 and 25.9 km s^{-1}, respectively. On the other hand, the average velocity difference with moving groups decreases with increasing multiplicity, from 28.6 km s^{-1} for triples to 17.9 km s^{-1} for hierarchies with $N > 4$.

Table 6
Kinematics of Multiple Systems within 100 pc

Sample	N	σ_U	σ_V (km s^{-1})	σ_W
All	866	37.0	31.1	35.5
Triple	665	39.4	33.8	39.8
Quadruple	158	28.4	19.8	13.3
$N > 4$	42	25.5	18.8	15.2
$P_{\rm out} > 10^7$ days	321	37.5	26.6	17.0
$P_{\rm out} < 10^4$ days	61	36.7	29.2	16.9

4.2. Compact Hierarchies

Although outer periods in triple and higher-order hierarchies are typically long, there are notable exceptions. Many tertiary components to *Kepler* EBs have periods of less than three years (Borkovits et al. 2016). The *Kepler* record so far belongs to J19499+4137 (KIC 5897826), with an outer period of only 33.9 days and an inner period of 1.767 days. However, a slightly shorter outer period of 33.07 days in J04007+1229 (λ Tau) has been known since 1982; the inner period of this B3V triple is 3.954 days; the period ratio is 8.37. Another compact hierarchy in the MSC is J16073−2204 (HD 144548, F7V); with periods of 33.9 and 1.63 days.

Hierarchies with outer periods shorter than three years can be discovered relatively easily by RVs or by ETV. The fact that such systems are much less frequent compared to those with longer periods reflects their real rareness. This has been noted in the 67 pc sample (Tokovinin 2014), where the shortest outer period of 1.75 yr among ∼500 hierarchies belongs to HIP 7601 (J01379−8259). The large number of triples with short outer periods discovered by *Kepler* is a selection effect. Although this discovery technique favors short outer periods, the majority of *Kepler* triples still have $P_{\rm out} \gtrsim 1000$ days.

There exist compact hierarchies with more than three components. The quintuple system VW LMi (J11029+3025) with an intermediate period of 355 days (Pribulla et al. 2008) contains 4 tightly packed solar-mass stars and the wide companion HIP 53969 at 340″ (estimated period 3 Myr). The *Gaia* parallaxes of the quadruple and the companion, 8.78 and 6.10 mas, respectively, differ significantly, but this discrepancy could arise from the photocentric motion with a 1-yr period.

4.3. Extreme Eccentricities

The two binaries with the largest reliably measured eccentricity of 0.975 are members of hierarchical systems. They are J15282−0921 (HD 137763 or GJ 586) and J18002+8000 (41 Dra, HD 166866). Both systems are quadruple. The inner eccentric binaries possibly was produced by the Lidov–Kozai cycles in hierarchies with large mutual orbit inclinations (Kiseleva et al. 1998; Naoz 2016). At such large eccentricities, the orbital periods cannot be much shorter than ∼3 yr without causing tidal orbit shrinking. So, if still larger eccentricities are to be discovered in the future, they will be found in binaries of even longer periods. Potential candidates for such searches can be selected from the MSC and monitored spectroscopically to catch short moments of passage through the periastron. In

GJ 586, Strassmeier et al. (2013) detected heating of the photosphere by tides at periastron.

4.4. Planar Systems and Resonances

Unlike planets in the solar system, the orbits of most binary stars have appreciable eccentricity, while orbits in triple systems are generally not confined to one common plane, showing only a modest alignment (Sterzik & Tokovinin 2002; Tokovinin 2017a). However, some hierarchies do resemble the solar system in this respect. The "planetary" quadruple HD 91962 (Tokovinin et al. 2015) consists of the outer visual binary with a period of 205 yr, the intermediate 9-yr spectroscopic and interferometric subsystem, and the inner 0.5-yr spectroscopic binary, in a 3-tier hierarchy. The period ratios are 23 and 18.97, and all orbits have moderate eccentricities of ~0.3. The angle between the outer and intermediate orbits is 11°.

The characteristic features of HD 91962 (modest eccentricity and period ratio, nearly coplanar orbits) are found in a number of other hierarchies, mostly comprised of low-mass stars (e.g., Tokovinin & Latham 2017). Such *planar* hierarchies could plausibly be sculpted by dissipative evolution of their orbits in a viscous disk.

Another slightly unusual characteristic of HD 91962 is the integer ratio of 18.97 ± 0.06 between the intermediate and inner periods. This suggests a mean motion resonance (MMR). However, a 1:19 resonance is very weak (hence unlikely), and alternatively, the integer period ratio could be a mere coincidence. In four low-mass triples with accurately measured period ratios, none of the ratios are an integer number, although they resemble HD 91962 in other aspects (Tokovinin & Latham 2017). So, the detection of MMRs in stellar systems remains controversial. Zhu et al. (2016) claimed that three companions to the eclipsing binary V548 Cyg found by ETV have period ratios of 1:4:12 (periods of 5.5, 23.3, and 69.9 yr) and are hence in the MMR. However, the interpretation of eclipse timing is sometimes controversial, so their result needs confirmation, e.g., by RV monitoring.

Resonances are commonly found in multi-planet systems (Fabrycky et al. 2014). They occur when an outer planet migrates inward in a disk, starts to interact dynamically with the inner planet, and is temporarily locked in an MMR. This mechanism can operate in stellar systems as well.

Intriguingly, there are quadruple systems where the ratios of the periods of two inner subsystems are a rational number. The only plausible interpretation is that both subsystems are in a MMR with the outer orbit. For example, Cagas & Pejcha (2012) found a doubly eclipsing quadruple system (J05484+3057) with periods of 1.20937 and 0.80693 days, in a 3:2 ratio. A similar situation occurs in the massive quadruple system HD 5980, where the inner eclipsing binary has a period of 19.266 days, while its tertiary component is itself a pair with a period of 96.56 days, exactly 5 times longer (Koenigsberger et al. 2014). Both close pairs in HD 5980 have very eccentric orbits.

4.5. Planets in Hierarchical Multiple Systems

Planets can orbit single stars as well as components of stellar binaries and multiples. In the latter case, a typical architecture is a triple system where the most massive primary component hosts one or several planets, while the wide secondary component is a close pair of low-mass stars. For example, the five-planet system *Kepler* 444 has a companion at 1.″8 that is a tight pair of M-dwarfs (Dupuy et al. 2016). Yet another example is 94 Cet (HIP 14954), where the primary F8V star hosts a planet, while the secondary pair of M-dwarfs is surrounded by a dust disk (Wiegert et al. 2016). A young star HD 131399 in Upper Scorpius has a planetary-mass companion Ab at a relatively large separation of 0.″8 from the main component Aa, challenging its stability in the 3.″2 outer system where Ba,Bb is a close pair (Veras et al. 2017). However, it turned out that this "planet" is actually a background star (Nielsen et al. 2017). Another young quadruple system in Taurus (J04417+2302) contains three L-type objects with masses between brown dwarfs and planets, while the main star A has an estimated mass of only $0.2\,\mathcal{M}_\odot$ (Bowler & Hillenbrand 2015). Discoveries of similar young multiples containing substellar bodies are likely to follow in the coming years.

The star HD 16232 has a planetary or brown dwarf companion with $P = 335$ days, as well as the 0.″54 visual companion discovered by Roberts et al. (2015). Together with HD 16246 it belongs to the quadruple system J02370+2439. Although quadruple systems with planets are rare, their number will likely increase in the near future.

5. Statistics

As noted above, the MSC is not based on a volume-limited sample, hence its contents do not reflect the real statistics of hierarchical systems; the statistics are distorted by the observational selection. Bearing this in mind, some statistical inferences can still be made from the MSC. For example, the author compared triple and quadruple systems under the assumption that selection affects both kinds of hierarchies in a similar way (Tokovinin 2008). The class of 2+2 quadruple systems, with components of similar mass and comparable inner periods, similar to the ϵ Lyrae, was singled out. Such quadruples often have outer periods shorter than 10^5 days.

The selection does not depend on the sense of rotation, allowing inferences about the relative orientation of orbits in triple systems (Sterzik & Tokovinin 2002; Tokovinin 2017a). There is a marked trend of co-alignment between the angular momentum vectors of the inner and outer orbits. This trend is stronger for compact triples with outer separation less than ~50 au, but the alignment disappears for outer systems wider than 10^3 au.

In this section, the ratio of periods (or separations) is discussed, based on the updated MSC.

5.1. Period Ratios

It is expected that all multiple systems (except possibly the youngest and widest ones) are dynamically stable. Several known criteria of dynamical stability (e.g., Harrington 1968) require that the ratio of the outer and inner periods, $P_{\rm out}/P_{\rm in}$, exceeds some threshold value that depends also on the outer eccentricity and on the masses. For example, the criterion of Mardling & Aarseth (2001) requires that in stable hierarchies with coplanar orbits $P_{\rm out}/P_{\rm in} > 4.7$.

Figure 7 compares periods at two adjacent hierarchical levels. It contains 2281 points (hierarchies with more than 3

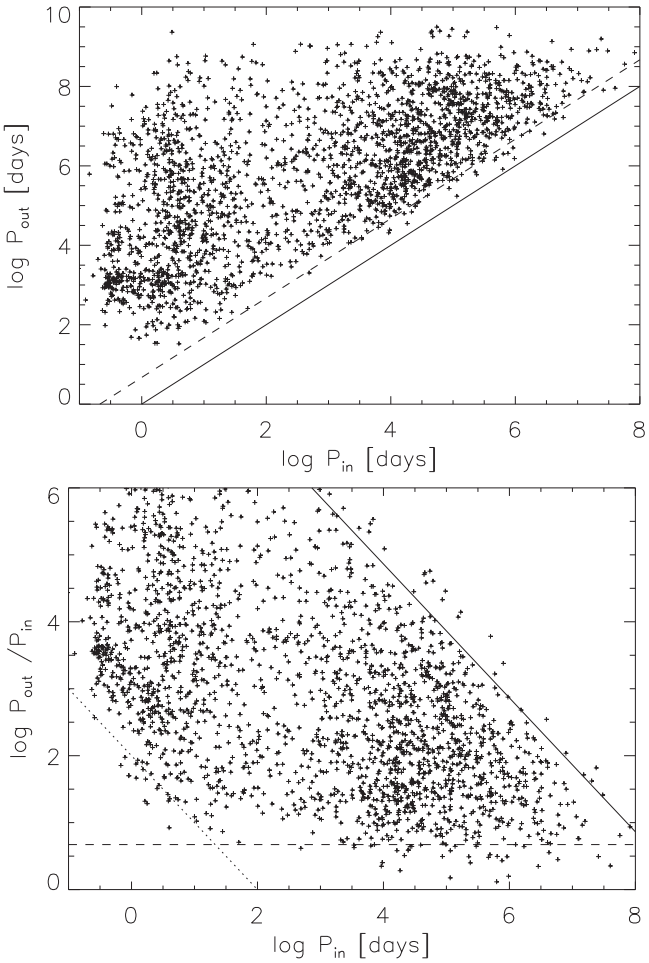

Figure 7. Top: periods at two adjacent hierarchical levels. The full line marks period equality, and the dashed line is the stability limit $P_{\rm out}/P_{\rm in} = 4.7$. Bottom: period ratio vs. inner period. The dashed line is the stability limit, and the full and dotted diagonal lines mark the outer periods of 2 Myr and 100 days, respectively.

components contribute more than 1 point). Long periods are estimated from the projected separations, so they are known within a factor of three or so. For this reason, some wide triples have their estimated period ratios $P_{\rm out}/P_{\rm in}$ below the dynamical stability limit (this issue is treated in Section 5.2). On the other hand, all hierarchies with actually measured orbital periods ($P_{\rm out} < 10^4$ days) do obey the stability criterion, and with a few exceptions, are elevated by at least ~0.5 dex above the dashed line in Figure 7. This trend is better visualized in the bottom plot of Figure 7. Short inner periods are associated with larger period ratios, meaning that such hierarchies are more stable dynamically, compared to wider ones.

The rarity of outer periods shorter than ~1000 days in the volume-limited 67 pc sample was noted by Tokovinin (2014) and is also apparent in the MSC through the nearly empty lower left corner in Figure 7. Short outer periods are therefore truly uncommon. This feature says something about the formation mechanisms of stellar systems: they likely had larger sizes at birth. In such cases, the short inner periods were produced by subsequent migration, while the outer systems migrated less, with some exceptions discussed in Section 4.2.

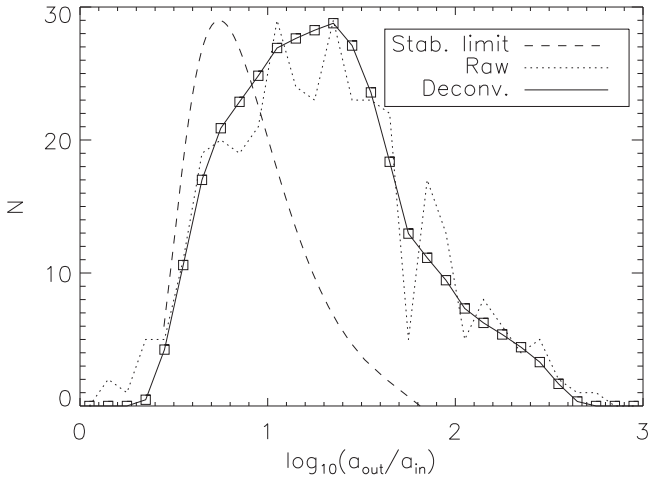

Figure 8. Distribution of the logarithmic ratio of projected separations x for 344 wide triple systems with $P_{\rm in} > 10^5$ days. The dotted line is the histogram, and the full line and squares is the distribution of the ratio of semimajor axes x_0 derived from this histogram by deconvolution. The dashed line is the assumed distribution of the critical axis ratio $\log_{10} R_0$.

5.2. Apparent Configurations of Wide Multiple Systems

Some visual multiples have apparently non-hierarchical configurations with comparable separations between their components (they are called *trapezia*). For example, the system J04519−3141 (HIP 22611 A,B and HIP 22604) contains three F- and G-type stars at separations of 99.″6 and 51.″9 that are definitely related, based on their common distances, PMs, and RVs. The orbital periods estimated from the projected separations, ~250 and ~109 kyr, are comparable and apparently violate the dynamical stability criterion (see the points below the dashed line in Figure 7). Here, we investigate whether such apparently unstable triples can be explained by projection effects. As the orbits of wide binaries are not known, the issue can be studied only statistically.

The dynamical stability criterion by Mardling & Aarseth (2001) is $a_{\rm out}/a_{\rm in} \geqslant R_0$ with

$$R_0 = 2.8(1 + q_{\rm out})^{1/15}(1 + e_{\rm out})^{0.4}(1 - e_{\rm out})^{-1.2}. \quad (3)$$

The critical ratio of semimajor axes R_0 depends on the eccentricity of the outer orbit $e_{\rm out}$ and on the outer mass ratio $q_{\rm out}$. In the following we neglect the weak mass-ratio dependence and assume that $e_{\rm out}$ has a bell-shaped distribution $f(e) = \pi/2 \sin(\pi e)$. This admittedly arbitrary assumption is needed to get an idea of the distribution of R_0. Our assumption is based on the fact that the average eccentricity of wide binaries containing inner subsystems is $e_{\rm out} \sim 0.5$, less than that for pure wide binaries (Tokovinin & Kiyaeva 2016). If the outer eccentricities are distributed linearly, $f(e) = 2e$, the resulting distribution of R_0 is broader.

We selected from the MSC 344 wide hierarchies of grades 4 and 5 with $P_{\rm in} > 10^5$ days and made a list of their outer and inner separations. When the inner orbit is known, its semimajor axis given in the MSC is replaced by the actual separation from WDS. These systems occupy the upper right corner of Figure 7. Let $x = \log_{10}(\rho_{\rm out}/\rho_{\rm in})$ be the logarithmic ratio of two separations. Its distribution in bins of 0.1 dex width is shown by the dotted line in Figure 8. Although this sample is not free from observational selection, the discovery of spatially

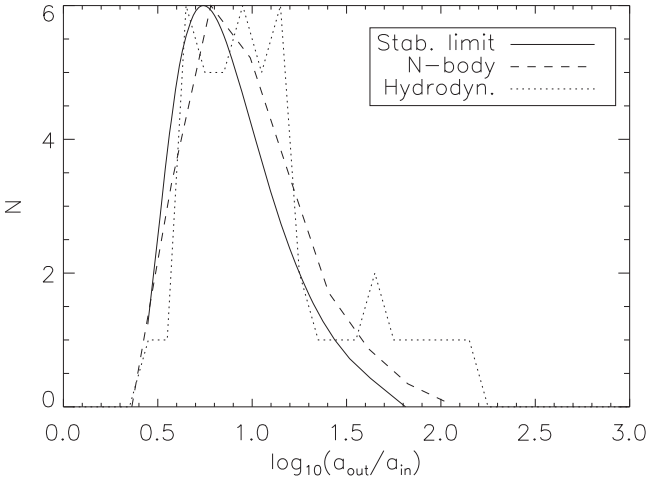

Figure 9. Separation ratio distribution for triple stars produced by scattering (Antognini & Thompson 2016) and in the hydrodynamical simulation of the collapsing cluster (Bate 2014). The solid line is the assumed distribution of the critical ratio $\log R_0$.

resolved wide hierarchies with comparable separations is relatively easy, so the leftmost part of the histogram should be a reasonable approximation of the real distribution.

The underlying distribution of the ratio of semimajor axes $x_0 = \log_{10} a_{\rm out}/a_{\rm in}$ is narrower than the distribution of x that is broadened by the projection and random orbital phases of both orbits. The broadening function is established by numerical simulation, assuming a realistic distribution of orbital eccentricities. As expected, deconvolution from the projection effects (see the Appendix) explains the small number of apparently unstable triples. The distribution of x_0 overlaps with the assumed distribution of $\log_{10} R_0$, so many wide triples can indeed be close to the dynamical stability limit. Nevertheless, the mean logarithmic ratio of semimajor axes $\langle x_0\rangle = 1.33$ dex is larger than the mean stability limit $\langle \log_{10} R_0\rangle = 0.93$ dex.

It is instructive to compare the separations in real wide triples with the theoretical predictions. Figure 9 shows the distribution of x_0 for hierarchical systems formed in the hydrodynamical simulations of a collapsing cluster. It uses the data from Table 4 of Bate (2014) for metallicities of 0.1, 1, and 3 times solar, a total of 50 points (the 17 dynamically unstable triples were excluded). The inner periods range from 100 days to ∼3000 yr, so these multiples are closer than the wide multiples in the field considered here; still, their distributions of x_0 are quite similar.

Antognini & Thompson (2016) performed a large series of N-body scattering numerical experiments. Triple systems were produced dynamically from binary–binary, triple-single, and triple-binary encounters. Data from their Figure 17 are used to compute the distribution of the ratio of the outer periastron distance to the inner semimajor axis, $\log_{10}[a_{\rm out}(1-e_{\rm out})/a_{\rm in}]$, plotted in Figure 9 as a dashed line. As this ratio is smaller than the ratio of the axes, the distribution of x_0 for dynamically formed hierarchies is slightly (by ∼0.3 dex) broader compared to the dashed line. It matches quite well the assumed distribution of the stability threshold R_0, illustrating the thesis of those authors that dynamically formed hierarchies are always "on the edge of stability" (see also Sterzik & Tokovinin 2002). Hierarchies formed in the hydrodynamical simulations of Bate (2014) have $\langle x_0\rangle = 1.14$ dex, being in this respect closer to the wide multiples in the field, $\langle x_0\rangle = 1.33$ dex.

6. Discussion

The number of known hierarchical stellar systems has tripled since the first MSC publication, mostly owing to the large observational programs conducted over the past two decades. At the same time, the diversity of the new MSC (e.g., the span of primary masses) has increased and new rare classes of hierarchies were found, as outlined in Section 4. Despite these advances, the census of hierarchical systems remains very incomplete; their number grows with distance as d^2, hence the apparent volume density drops as d^{-1} even in the close vicinity of the Sun. Figure 3 illustrates some aspects of this observational selection. Thousands of hierarchical systems within 100 pc still wait to be discovered.

Although hierarchical multiples can be interesting objects in their own right (e.g., to study dynamics or to measure stellar parameters), their role in revealing the origins of stellar systems cannot be underestimated. The MSC helps here by offering a large statistical sample (albeit burdened by the selection). The structure of the period–period diagram in Figure 7 (bimodal distribution of inner periods, rarity of short outer periods, distribution of the period ratios) appears to be linked to the formation and early evolution of stellar systems. The MSC is also a source of unusual objects highlighting particular aspects of their formation, e.g., hierarchies with an architecture resembling planetary systems. The accreting proto-triple system discovered with ALMA by Tobin et al. (2016) may eventually become a nearly coplanar planetary-like triple. However, further discussion of formation mechanisms of binary and multiple stars is outside the scope of this work.

The MSC is based on the work of several generations of observers who patiently collected data for the benefit of future science, rather than for immediate use. Compiling and updating the binary-star catalogs is an often forgotten but essential activity. Three of the major catalogs used here (WDS, VB6, INT4) are maintained at the USNO, while SB9 is hosted at the Université Libre de Bruxelles. This work also used the SIMBAD and VIZIER services operated by Centre des Données Stellaires (Strasbourg, France) and bibliographic references from the Astrophysics Data System maintained by SAO/NASA. Comments from the referee helped to improve the paper.

Appendix
Deconvolution of Projected Separations

We simulated a large number of binaries with a unit semimajor axis, a random orbital phase and orientation, and a given eccentricity distribution. The latter is assumed to be either thermal, $f(e) = 2e$, or bell-shaped, $f(e) = \pi/2 \sin(\pi e)$. The logarithmic ratio of the separations of two such random binaries, $x = \log_{10}(\rho_1/\rho_2)$, is distributed symmetrically around zero. An analytical formula was chosen to approximate the cumulative distribution of x. Its derivative gives the approximate form of the broadening function due to projection,

$$P(x) \propto {\rm e}^{-2.8|x|}\,(2.8 + 2a + 2.8ax^2)/(1 + ax^2). \qquad (4)$$

Here, the parameter $a = 4$ is valid for the thermal eccentricity distribution, while $a = 2$ gives a good approximation for the bell-shaped eccentricity distribution. We used $a = 4$ in the following.

The histogram of the logarithmic separation ratio x, h_i ($i = 1 \ldots M$ is the bin number), is related to the histogram of the logarithmic semimajor axis ratios x_0, H_i, by the convolution equation with the kernel P. In discrete formulation, $\boldsymbol{h} = A \cdot \boldsymbol{H}$, where the $M \times M$ matrix A describes the convolution: $A_{i,j} = C\ P(\Delta x(i - j))$. Here, Δx is the bin width of the histogram and the constant C normalizes the sum of each line to one. Direct inversion of this equation to derive **H** from **h** leads to the amplification of the statistical noise, hence some regularization is needed. We look for a smooth distribution **H**. It is found by minimizing the merit function

$$\min\left[\sum_{i=1}^{M}[h_i - (A \cdot \boldsymbol{H})_i]^2 + \alpha \sum_{i=1}^{M-1}(H_i - H_{i+1})^2\right] \qquad (5)$$

with a small regularization parameter α. The full curve in Figure 8 was computed with $\alpha = 0.2$, using $M = 30$ bins and $\Delta x = 0.1$. The model histogram $A \cdot \boldsymbol{H}$ is compatible with the data $\boldsymbol{h}$, considering its Poisson statistics. Therefore, the chosen parameter α is not too large.

ORCID iDs

Andrei Tokovinin https://orcid.org/0000-0002-2084-0782

References

Antognini, J. M. O., & Thompson, T. A. 2016, MNRAS, 456, 4219
Bate, M. 2014, MNRAS, 442, 285
Borkovits, T., Hajdu, T., Sztakovics, J., et al. 2016, MNRAS, 455, 4136
Bowler, B. P., & Hillenbrand, L. A. 2015, ApJL, 811, 30
Cagas, P., & Pejcha, O. 2012, A&A, 544, L3
D'Angelo, C., van Kerkwijk, M. H., & Rucinsky, S. M. 2006, AJ, 132, 650
De Rosa, R. J., Patience, J., Wilson, P. A., et al. 2014, MNRAS, 437, 1216
Dieterich, S. B., Henry, T. J., Golimowski, D. A., et al. 2012, AJ, 144, 64
Dupuy, T. J., Kratter, K. M., Kraus, A. L., et al. 2016, ApJ, 817, 80
Eggleton, P. P. 2009, MNRAS, 399, 1471
Elliott, P., & Bayo, A. 2016, MNRAS, 459, 4499
Fabrycky, D. C., Lissauer, J. J., Ragozzine, D., et al. 2014, ApJ, 790, 146
Gaia Collaboration, Brown, A. G. A., Vallenari, A., Prusti, T., et al. 2016, A&A, 595, 2
Harrington, R. S. 1968, AJ, 73, 508
Hartkopf, W. I., Mason, B. D., & McAlister, H. A. 2001, AJ, 122, 3480
Hartkopf, W. I., Mason, B. D., & Worley, C. E. 2001, AJ, 122, 3472
Kiseleva, L. G., Eggleton, P. P., & Mikkola, S. 1998, MNRAS, 300, 292
Koenigsberger, G., Morrell, N., Hillier, D. J., et al. 2014, AJ, 148, 62
Law, N. M., Dhital, S., Kraus, A., et al. 2010, ApJ, 720, 1727
Liao, W.-P., & Quian, S.-B. 2010, MNRAS, 405, 1930
Mardling, R. A., & Aarseth, S. J. 2001, MNRAS, 321, 398
Mason, B. D., Wycoff, G. L., Hartkopf, W. I., Douglass, G. G., & Worley, C. E. 2001, AJ, 122, 3466 (WDS)
Muterspaugh, M. W., Lane, B. F., Kulkarni, S. R., et al. 2010, AJ, 140, 1657
Naoz, S. 2016, ARA&A, 54, 441
Nielsen, E. L., De Rosa, R. J., Rameau, J., et al. 2017, AJ, 154, 218
Pecaut, M. J., & Mamajek, E. E. 2013, ApJS, 208, 9
Pourbaix, D., Tokovinin, A. A., Batten, A. H., et al. 2004, A&A, 424, 727
Pribulla, T., Baluďansky, D., Dubovsky, P., et al. 2008, MNRAS, 390, 798
Raghavan, D., McAlister, H. A., Henry, T. J., et al. 2010, ApJS, 190, 1
Ressell, H. N., & Moore, C. E. 1940, Masses of Stars (Chicago, IL: Univ. Chicago)
Roberts, L. C., Jr., Tokovinin, A., Mason, B. D., et al. 2015, AJ, 149, 118
Sana, H., Le Bouquin, J.-B., Lacour, S., et al. 2014, ApJS, 215, 15
Sterzik, M., & Tokovinin, A. 2002, A&A, 384, 1030
Strassmeier, K. G., Weber, M., & Granzer, T. 2013, A&A, 559, 17
Tobin, J. J., Kratter, K. M., Persson, M. V., et al. 2016, Natur, 538, 483
Tokovinin, A. 1997, A&AS, 124, 75
Tokovinin, A. 2004, RMxAC, 21, 7
Tokovinin, A. 2005, HiA, 13, 992
Tokovinin, A. 2008, MNRAS, 389, 925
Tokovinin, A. 2014, AJ, 147, 86
Tokovinin, A. 2017a, ApJ, 844, 103
Tokovinin, A. 2017b, MNRAS, 468, 3461
Tokovinin, A., & Kiyaeva, O. 2016, MNRAS, 456, 2070
Tokovinin, A., & Latham, D. W. 2017, ApJ, 838, 54
Tokovinin, A., Latham, D. W., & Mason, B. D. 2015, AJ, 149, 195
Tokovinin, A., Mason, B. D., & Hartkopf, W. I. 2010, AJ, 139, 743
Tokovinin, A., Thomas, S., Sterzik, M., & Udry, S. 2006, A&A, 450, 681
van Leeuwen, F. 2007, A&A, 474, 653
Veras, D., Mustill, A. J., & Gänsicke, B. T. 2017, MNRAS, 465, 1499
Wiegert, J., Faramaz, V., & Cruz-Saenz de Miera, F. 2016, MNRAS, 462, 1735
Zasche, P., Uhlár, R., Slechta, M., et al. 2012, A&A, 542, 78
Zhou, X., Quian, S.-B., Zhang, J., et al. 2016, ApJ, 817, 133
Zhu, L.-Y., Zhou, X., Hu, J.-Y., et al. 2016, ApJ, 151, 107